Experimental aspects of biological X-ray absorption spectroscopy

Isabella Ascone,[a]* Wolfram Meyer-Klaucke[b] and Loretta Murphy[c]

[a]LURE, Bâtiment 209E, Université Paris-Sud, 91898 Orsay CEDEX, France, [b]EMBL, c/o DESY, Notkestrasse 85, Geb 25A, 22607 Hamburg, Germany, and [c]Daresbury Laboratory, Warrington WA4 4AD, UK.
E-mail: isabella.ascone@lure.u-psud.fr

Spectroscopic techniques, like X-ray absorption spectroscopy, will provide important input for integrated biological projects in genomics and proteomics. This contribution summarizes technical requirements and typical set-ups for both simple and complex biological XAS experiments. An overview on different strategies for sample preparation is discussed in detail. Present and future BioXAS spectrometers are presented to help potential users in locating the spectrometer required for their biological application.

Keywords: BioXAS; metalloproteins; experimental set-up; macromolecules.

1. Introduction

X-ray absorption spectroscopy (XAS) has been widely used in many areas of science during the last 20 years. The feasibility of using this technique for biological systems was demonstrated in the first fluorescence experiment (Jaklevic *et al.*, 1977). Subsequently, several reviews highlighted its contribution to the characterization of metal centres in biological systems (Cramer, 1988; Garner & Charnock, 1993; Hasnain & Hodgson, 1999). Nevertheless, biological X-ray absorption spectroscopy (BioXAS) has demanding experimental requirements that until 1990 were available at only a few XAS beamlines worldwide. In 1985, Fiamingo & Alben (1985) pointed out the necessity to improve the experimental conditions in order to extract reliable information from BioXAS data; however, some of these have been developed only recently. In particular, there are two major technological advances that have improved BioXAS measurements:

(i) The source intensity of second-generation machines has been increased by insertion devices or focusing optics while third-generation machines produce high-intensity and focused X-ray sources. This feature allows us to increase the signal, and to decrease the biological sample concentration and/or sample volume.

(ii) Fluorescence detectors, which are essential for measurements on dilute samples, are now much more efficient and are continually improving.

These technical improvements have increased the quality of BioXAS measurements: the information obtained is more reliable as the *k*-range of the EXAFS signal is extended.

This paper will firstly present the typical biological XAS experimental set-up and then summarize the different elements such as source, monochromator, detectors and sample environment devices. Particular attention will be given to metalloprotein studies. The aim is to give the reader, interested in studying a protein metal site, some help in choosing the experimental set-up and the appropriate sample environment.

2. A typical biological XAS experiment

Important scientific questions, like the structural and electronic characterization of metal sites, can be performed on BioXAS beamlines using a layout described in the following paragraphs.

Synchrotron beamline. A basic X-ray spectroscopy station consists of a scanning high-resolution monochromator, a beam monitor and a signal detector. The signal is detected in transmission or in fluorescence mode. In the first case, two ionization chambers are generally used as detectors, to measure the X-ray flux before (I_o) and after (I_t) the sample. In the second detection mode, specific for diluted samples (absorber concentration <1%), a detector is placed perpendicular to the beam to measure the fluorescence signal (I_f).

Sample. BioXAS can be measured on samples in any state, *e.g.* room temperature or frozen solution at liquid-nitrogen or helium temperatures, single crystals (Scott *et al.*, 1982), crystalline slurry (Ascone *et al.*, 1997), all or part of an organism (Kramer *et al.*, 1986). The choice of sample state depends entirely on the robustness of the sample and the scientific question you are trying to answer. However, typically frozen solutions are studied in order to lower the thermal disorder and minimize the radiation damage. Typically, the metalloprotein (metal concentration *ca* 1–5 m*M*, volume 10–120 µl) is loaded in a plastic cell with plastic film covering the central aperture and frozen in liquid nitrogen. The sample is frequently measured at either liquid-nitrogen or helium temperatures *via* the use of cryostats. In some cases cryoprotectants need to be added to the protein solution. The materials used to construct the sample cell and sample environment must be free of significant metal content relative to the concentration of the sample itself.

3. Characteristics of the X-ray source

The X-ray absorption cross section of a metalloprotein is particularly low compared with the absorption of samples frequently used for material science experiments. Metal is bound to one or more amino acid chains having a high molecular weight (10–100 kD or more). Moreover, the protein is diluted in an aqueous solution. The XAS signal (detected by fluorescence) is proportional to the intensity of the incident beam. Therefore BioXAS strongly depends on intense insertion-device sources which are available at second- and third-generation synchrotron beamlines. In contrast to other powerful techniques, like protein crystallography, BioXAS cannot be performed on laboratory X-ray sources such as rotating anodes or X-ray tubes. Thus, even the preliminary tests to prepare a BioXAS experiment have to be performed at a synchrotron centre. Dedicated beam time is necessary in order to optimize the conditions for sample concentration, its susceptibility to radiation damage or for kinetics.

The intensity of the XAS signal depends on several parameters: the characteristics of the machine (critical energy, insertion devices, current *etc.*), the energy of the absorption edge of the metal of interest, the focusing optics and the quality of the fluorescence detector available. The intensity and size of the beam irradiating the sample will directly effect the minimum usable sample concentration and volume. At present, two major types of beamlines exist: (*a*) high-flux beamlines on insertion devices (undulators, wigglers or wavelength shifters) (Gauthier *et al.*, 1999; Solé *et al.*, 1999; Tanida & Ishii, 2001), and (*b*) low-flux beamlines at bending magnets. Both types have advantages and disadvantages for BioXAS experiments.

A high-flux beamline reduces considerably the quantity of protein required for XAS measurements (Ranieri-Raggi *et al.*, 2003); sample volumes of 10–20 µl with metal concentrations of about 50–100 µ*M* are feasible but with a risk of photoreduction altering the metal site.

This issue has not been completely addressed, as the number of biological studies on this type of set-up is relatively small. Nevertheless, such beamlines are ideal for the high-throughput studies required for structural genomics and later for the analysis of the metallome as this set-up reduces the data-acquisition time as well as the quantity of the sample.

Bending-magnet beamlines typically require sample volumes of 25 to 100 μl at a metal concentration of at least 0.5 mM. For the same exposure time, the radiation dose on the samples is much lower and the beamlines are optimized for an efficient use of the fluorescence radiation. Therefore only a small fraction of the metal centers will be reduced during the data acquisition, but samples must always be monitored for radiation damage. As each protein has a specific behaviour under irradiation, tests on protein stability should be routinely performed.

The two types of beamlines are suitable for different BioXAS projects. Whereas the bending-magnet beamlines mainly serve the user community for standard experiments, the high-flux beamlines are best suited for experiments on ultra-dilute samples. At undulator and wiggler beamlines, time-resolved XANES can be performed in the 50 ms time range.

The most advanced third-generation synchrotrons have small source size, which is an important characteristic in order to obtain XANES spectra with high experimental resolution ($\Delta E/E \simeq 5 \times 10^{-5}$). For protein solutions at concentrations <50 μM, XANES is the only region of XAS spectra with a sufficiently high signal-to-noise ratio. XANES and pre-edge regions are sensitive to the structural and electronic properties of the metal site [see Kau *et al.* (1987) and other contributions in this issue]. Description of the metal site at the molecular level of detail is essential for investigating the reactivity properties. The combination of high-resolution XANES data and theoretical advances will increase information obtained from spectra.

4. Monochromators and optics

Monochromators allow selection of the energy required to excite the L- or K-edges of biologically relevant elements. The set of elements which strongly interact with proteins, acting as co-factors or as part of substrate binding/utilization sites, is relatively small. It includes Mg, Al, Ca, all members of the first transition series (excluding Sc, Ti), Br, Se, Mo, W, Cd and Hg. Nevertheless, the number of proteins interacting with a metal is high (Holm *et al.*, 1996).

Most BioXAS experiments are performed at energies higher than 5 keV, above which the K-edge absorption of elements having an atomic number greater than 22 (titanium) occurs.

Monochromatic light is produced through utilization of Bragg reflection(s) on perfect crystal(s). Monochromator crystals are mostly Si(111), Si(220), Si(311) and Ge(111), in predominantly double-crystal configuration. The choice of crystal depends on the required energy resolution and intensity. For instance, Ge(111) has poorer resolution but higher flux than Si(111), and Si(311) has a higher energy resolution but a lower flux than Si(111).

Owing to lattice properties of the crystals (2d spacing of beryl 1010 is 15.954 Å), 0.8 keV is the lower limit of a double-crystal monochromator which is frequently used for hard X-ray beamlines. Spectra of diluted biological samples have a low signal-to-noise ratio and require a highly stable and an optimized experimental set-up. The quality of spectra is very sensitive to intensity variations in the incident X-ray flux (I_0) over a small energy range. Higher-order harmonic reflections, electronic noise or insufficient mechanical/thermal stability of the optics in the energy range of the scan may produce I_0

Table 1
Bragg angles required to select different energies with Si(111) and Si(311) crystals.

Energy (keV)	2.1	3.1	4.1	5.1	8	9	10
$\theta_{Si(111)}$ (°)	69.1	39.1	28.8	22.8	14.3	12.7	11.4
$\theta_{Si(311)}$ (°)			67.5	47.9	28.4	24.9	22.3

irregularities. Thus glitches are produced in an XAS spectrum when I_f is not correctly normalized by I_0 (see §5).

In the energy range 2–5 keV, the mechanics of the monochromator have to be particularly stable, as the monochromator angular movement for an XAS scan is large. For example, with Si(111) the angle variation between 2.1 and 3.1 keV is 30°, while the angle variation between 9 and 10 keV is about 1°. Table 1 presents the Bragg angles required to monochromize the beam for selected energies using Si(111) or Si(311) crystals.

The elements probed in the 2–5 keV energy range are P, S, Cl and Ca. Phosphorus K-edge XAS of biological systems has been performed at SSRL using a Ge(111) monochromator (George, 1993).

Owing to the rapid degradation of monochromator crystals in the 1–2 keV energy region, elements like Mg and Al have not been frequently studied (George, 1993). Moreover, the crystals for this energy domain contain elements which limit the energy range. Beryl is used in the energy range 0.8–1.55 keV as it contains Al (K-edge at 1559.6 eV) and Si (K-edge at 1839 eV) while α-quartz contains Si (Lagarde & Flank, 2002). The use of a YB$_{66}$ monochromator crystal (energy range 1.1–2.1 keV), suitable for the Mg K-edge, was proposed only in 1993 (Rowen *et al.*, 1993).

At energies lower than 1 keV, K-edge absorption of C (284.2 eV), N (409.9 eV), O (534.1) and L-edges of first-series transition elements are found.

Carbon, nitrogen and oxygen are present in abundance in biological molecules with a variety of atomic environments; thus only average environments can be deduced which in most cases is of little biological value. L-edges contain information on the spin state and oxidation states of the above-mentioned transition metals (Wang *et al.*, 2001; George *et al.*, 1993). The energy resolution of L-edge spectra is three- to fourfold higher than that at the K-edge, allowing the detailed observation of transitions (ligand field splitting of d orbitals) and the probing of metal–ligand covalency. The character of the metal–ligand bond can also be explored by studying the ligand K-edge spectra. Sulfur K-edge XAS has been used to investigate the covalency of the Cu—S bond at the active site of plastocyanin (Shadle *et al.*, 1993; Pickering *et al.*, 1998; Yu *et al.*, 2001).

The energy of the absorption edge is frequently used to determine the oxidation state of metals in proteins. For accurate determination of the energy scale, it is highly desirable to have two independent measurements of the energy: one from the monochromator angular position and the other from a physical measurement of the energy during the scan. This can be accomplished in several ways using the remaining intensity of the beam transmitted by the sample. The absorption of a reference sample (frequently a metal foil) could be monitored simultaneously *via* a transmission measurement using a fraction of the beam which is not absorbed by the sample.

Alternatively the reflections of a static Si crystal could be detected by an angular-resolved detector set-up over the full energy range (Pettifer *et al.*, 1985). Refinement of a regression curve allows the absolute calibration and a correction of mechanical inaccuracies.

Beam focusing in the vertical direction may be performed using mirrors. Recent advances in monochromator design have included the use of sagittal (horizontal) focusing monochromators for biolo-

gical samples which reduce the size of the beam footprint, and hence the sample size and volume, while dramatically increasing the X-ray flux on the sample. There are a number of different designs of sagittal monochromator worldwide. Fig. 1 shows 3.3 mrad radiation (equivalent to 43 mm) focused onto a spot size of 1.15 mm (FWHM) using a Si(111) sagittal monochromator on a bending magnet of a second-generation machine, SRS. A similar monochromator has recently been implemented on the 6 T wavelength-shifter XAFS instrument 16.5 from which an example of data quality is shown for a submillimolar Zn sample of volume 40 µL.

5. Detectors

Many XAS applications concern the field of materials science which includes a large number of samples having high concentration (>2–3%) of the absorbing element. With this kind of sample, measurements can be performed in transmission mode, with two ionization chambers, which detect signals incident on, and transmitted by, the sample.

Dilute samples, like proteins, require the detection of the XAS signal in fluorescence mode, which allows a better signal-to-noise ratio in spectra. Particular attention should be given to the choice of the beam monitor. If I_0 and the fluorescence detector do not have an equivalent response, *i.e.* are non-linear to the beam instability and/or

intensity variations in a scan, the spectra may exhibit artefacts. One of the methods proposed to improve linearity is to monitor the beam intensity with a Si diode, which detects the scattering of a foil (Retournard *et al.*, 1986; Gauthier *et al.*, 1999). After the first X-ray fluorescence experiment (Jaklevic *et al.*, 1977), instruments with different working principles have been developed: inorganic (Cramer *et al.*, 1978) and organic (Powers *et al.*, 1981) scintillation detectors, fluorescence detection using gases (Lytle *et al.*, 1984), large-surface Si diodes (Retournard *et al.*, 1986), multi-element energy-resolved detectors (Cramer *et al.*, 1988).

Multi-element semiconductor (Si or Ge) detectors have been commercially distributed, associated to specific electronic chains, by several companies. During the last decade, multi-element Ge detectors have become the standard equipment for most biological XAS projects. The recent high-dilution XAS beamline at SPring-8 (Japan) has been equipped with a 19-element solid-state detector (Tanida & Ishii, 2001). A low-profile monolithic nine-element Ge detector has been specifically developed to be easily incorporated into complex sample stages such as those used for performing protein single-crystal XAS studies (Derbyshire *et al.*, 1999). This approach is based on monolithic Ge detectors lowering the dead area between different detector elements. In this case, the efficiency is increased from 36% (in standard multi-element detectors) to greater than 90%.

Standard multi-element Si and Ge detectors are saturated by the intensity of the photon flux of third-generation machines. Specific devices are required to benefit from the photon flux increase, reducing the exposure time and the sample concentration. Different approaches have been proposed to overcome this issue, such as a synthetic multilayer detector (Zhang *et al.*, 1998), a silicon pnn+ photodiode (Gauthier *et al.*, 1999) and silicon drift multi-detectors associated with specific electronics, developed at ESRF (Gauthier *et al.*, 1996) or at HASYLAB (Kappen *et al.*, 2002).

6. Sample preparation and environment

In a BioXAS experiment the amount of sample required for a measurement is a critical point. Most of the proteins (especially protein mutants) are not available commercially and often require delicate purification steps before using in an XAS experiment. The BioXAS sample cells are designed in order to reduce the amount of sample required for one measurement. Minimization of the quantity of protein used is also possible through the use of a high-flux beamline (see §3).

There are several different types of sample environment that are now in use for BioXAS measurements. In many experiments the data are collected on cryogenically cooled samples (see §6.6). Other types of sample environments have recently been developed, *e.g.* electrochemical cells, high-pressure cells and combined stopped-flow cells (see below). These are designed to take into account the technical constraints related to biological samples.

6.1. Sample reactivity

XAS can provide structural details on metal coordinations in solution, important information when elucidating the structural basis of biological mechanisms (see, for example, Shu *et al.*, 1997). The analysis of intermediate states can be achieved either by improving the time resolution of the spectrometer, for example with a quick-EXAFS set-up (Richwin *et al.*, 2001), or stabilizing a particular state at low temperature through freeze-quench techniques. For example, two intermediates in a ferritin reaction with Fe^{2+} and O_2 have been recently trapped by rapid freeze quench at 25 ms and at 1 s (Hwang *et al.*, 2000).
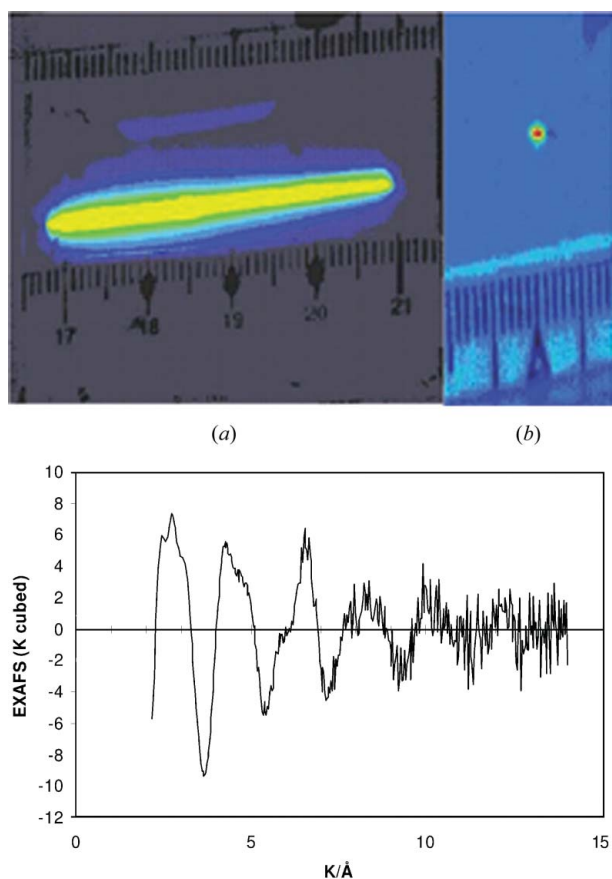

Figure 1
Upper panel: images of an X-ray beam from station 7.1, Si(111) monochromator (*a*) unfocused, (*b*) sagittally focused (beam footprint FWHM = 1.15 mm). (Kindly supplied by K. C. Cheung, Daresbury Laboratory, UK). Lower panel: single EXAFS scan of 40 µL 0.8 m*M* Zn in Zn β-lactamase. Station 16.5, located at the 6 T wavelength shifter (in sagittal mode). (Both from SRS Daresbury Laboratory, UK.)

Studies of proteins performed in quasi-physiological solution are highly desirable, but under these conditions proteins are quite reactive. *In situ* equipment for controlling and/or monitoring physico-chemical characteristics of the sample during measurements (UV, IR, Raman spectrometers) have a double role. Firstly, these devices allow verification of the absence of unwanted reactions during the characterization of a particular protein state, and, secondly, they help characterize kinetic reactions and link them to structural changes monitored by XAS. Cells with a system assuring the circulation and the renewal of the solution during the experiment (like a stopped-flow system) are useful for removing radiation-damaged materials or for time-resolved experiments.

An on-line tuning laser completes the equipment for experiments requiring photolysis-induced reaction intermediates (Haumann *et al.*, 2002). For such applications, cells should have a transparent aperture to enable laser irradiation.

In order to study *in situ* kinetic reactions, a high-brilliance source coupled to a quick-XAS set-up is highly desirable.

A combined stopped-flow/fluorescence EXAFS cell has been developed at Daresbury (L. Murphy, personal communication) where one face of a standard stopped flow cell has been modified to incorporate an X-ray transparent window, thus permitting simultaneous measurement of the optical and XAS fluorescence spectra.

At EMBL Outstation (Hamburg), kinetic reactions are being studied with a time resolution of about 50 ms per scan (350 eV) using a piezo quick-XAS set-up. An example monitoring the photoreduction of purple acid phosphatase from kidney bean is depicted in Fig. 2.

6.2. Sample in the crystalline state

There have been relatively few single-crystal XAFS studies on protein crystals (Bianconi *et al.*, 1985; Scott *et al.*, 1982; Flank *et al.*, 1986; Chen *et al.*, 1993). Synchrotron radiation sources provide highly polarized X-rays which, with suitable crystals, can be used to probe the metal sites at orientations chosen to enhance the contribution of specific backscatterers to the XAFS spectrum.

A study on oriented single crystals of nitrogenase in 1986 (Flank *et al.*, 1986) was used to investigate the geometry and orientation of the Mo, Fe and S clusters within the Mo–Fe protein many years prior to
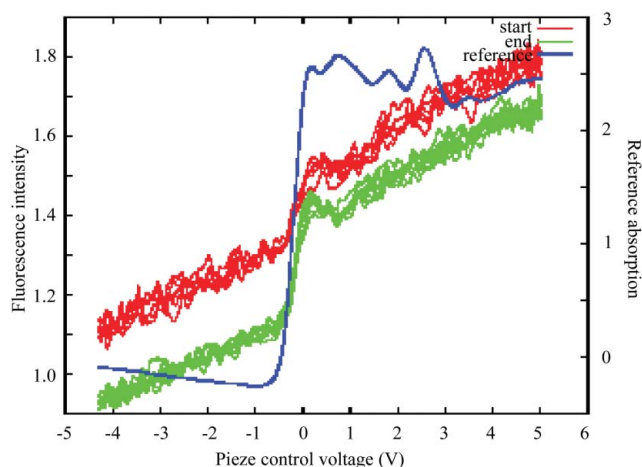
Figure 2
Fluorescence XANES spectrum recorded at a second-generation wiggler beamline by means of a photodiode. The iron concentration in the sample was about 0.5 mM. First (red) and last spectra (green) of Fe K-edge fluorescence; reference sample for calibration shown in blue. (M. Richwin *et al.*, HASYLAB annual report 2001.)

determination of the X-ray crystallographic structure at medium resolution.

If single crystals of a suitable size are not available, it is also informative to study crystalline slurries. Crystalline slurry is a sample state formed by randomly oriented microcrystals. In metalloprotein studies, this preparation allows one to correlate the electronic state of metals in solution and in the crystalline state (Ascone *et al.*, 1997). To avoid polarization effects, a large amount of microcrystals (10–100 µm) have to be irradiated; for this reason a highly focused beam is not suitable.

6.3. Temperature and pressure range for protein studies

Each family of proteins has a specific temperature and pressure range of stability. In any case, the extreme values of temperature and pressure are low compared with those used in materials science studies. Ovens reaching more than 1200 K and pressure devices achieving 6 GPa are currently used at XAS beamlines, but these devices are not suited for life science experiments.

High-pressure-adapted organisms, referred to as piezophiles, have optimal reproduction rates at pressures greater than 0.1 MPa, and hyperpiezophiles possess optimal growth rates at pressures >60 MPa (Bartlet, 2002).

The maximum temperatures at which proteins exert their biological activity are relatively low. The most extreme of hyperthermophiles, organisms which inhabit submarine hydrothermal vents, grow in the range 353–383 K (Madigan & Oren, 1999).

As temperature is a critical parameter for preserving proteins from denaturation, cells with temperature control (cryostat, thermostatic bath) are essential. Low temperatures are currently used in crystallography or NMR protein studies to preserve the sample. In XAS studies, cryostats cooling the sample also increase the signal quality due to lower dynamic disorder. This procedure is not exempt from risk; it is well known that some proteins lose, reversibly or irreversibly, their activity as temperature decreases. One of the causes of the cryoinactivation is related to the stability of protein folding at low temperatures.

When preparing a protein sample, the possibility of cold denaturation has to be taken into account, as described in §6.6.

Pressure effects on biological systems are actually widely studied. A recent volume [see Banly *et al.* (2002), and all the reviews in the same volume] illustrates the role that this thermodynamic variable plays in various processes: intermolecular protein reactions, pressure-induced conformational changes, unfolding.

Depending on the systems, pressures higher then 0.4 GPa lead to the unfolding of proteins in solution. It has been recently demonstrated that some proteins in the crystalline state are more stable at high pressure than was expected, extending the pressure range of interest. Three-dimensional protein structure is preserved up to about 0.9 GPa in tetragonal crystals of hen egg-white lysozyme and at least 1 GPa in orthorhombic crystals of bovine erythrocyte Cu, Zn superoxide dismutase (Fourme *et al.*, 2001, 2002).

Low-pressure environments are also useful for BioXAS. Elastic effects on the three-dimensional protein structure in solution occur in the range 0.1–0.4 GPa (1 bar to 4 kbar). Pressure variations in this range permit the investigation of the fractional population of conformational substates. XAS could contribute to the structural characterization of conformational substates, having similar structures, and of pressure-denatured states.

The only attempt using XAS to study protein behaviour under pressure has been performed using a Paris–Edinburgh press coupled to a fluorescence detector (Ascone, Cognigni *et al.*, 2000). This device,

designed to achieve pressures higher than 0.2 GPa (2 kbar), is not appropriate for modulating pressure in the 0.1–0.4 MPa range. A device for studying the reversible pressure effects in proteins should be specifically developed, as the sample holder of a Paris–Edinburgh press is irreversibly deformed by pressure, thus changing the pathlength of the sample being studied.

6.4. X-ray damage

Photoreduction of the metal site is a possibility that should not be neglected in planning BioXAS or protein diffraction experiments. There is no general rule for predicting the behaviour of a protein during irradiation. The photoreduction process strongly depends on the metal site, on exposure time and on the intensity of the source. Two examples concerning two proteins (cytochrome c and Cu, Zn superoxide dismutase) having different metal site stability illustrate this fact.

At the intense wiggler beamline of SSRL (SPEAR), the first 23 spectra of oxidized cytochrome c recorded at the Fe K-edge are unchanged during data acquisition. Starting from the 24th spectrum, changes in the edge energy appear. The 39th spectrum presents an energy shift of 0.5 eV compared with the edge energy of the XANES initially recorded (Cheng *et al.*, 1999). The energy shift indicates cytochrome c photoreduction.

The same system is stable on the DCI-D21 bending-magnet source for at least 48 h (I. Ascone, personal communication). No sign of photoreduction is detected with the DCI source for long beam exposure times. The SPEAR source is more suitable for studying this system as the signal to noise obtained by averaging 23 spectra is better than that obtainable at DCI.

Bovine oxidized Cu, Zn superoxide dismutase is stable at room temperature during the recording of at least four spectra (4 h) with the bending magnet DCI-D21 (LURE, Orsay). The same sample at room temperature has been exposed to the intense undulator beam of ID26 at ESRF. In 1 s the protein is partially reduced, as shown in Fig. 3 (I. Ascone, personal communication).

The stability of a similar copper metal site is longer at Hamburg EMBL Outstation. At 20 K, a polycrystalline sample of engineered monomeric human Cu, Zn superoxide dismutase triple mutant F50E/G51E/E133Q has been exposed to the synchrotron beam for 18 h, recording XAS spectra at different exposure times (Ferraroni *et al.*, 1999). After 40 min of irradiation by the Doris III bending-magnet
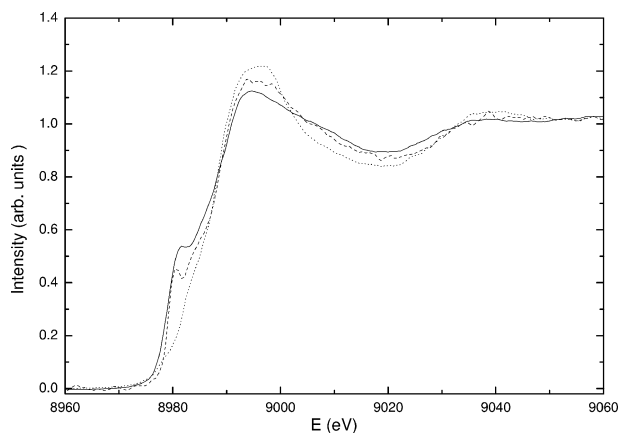
X-ray beam, the peak assigned to the $1s \rightarrow 4p$ transition, diagnostic for site reduction, appears on the second spectrum. After 18 h the photoreduction of the copper metal site has progressed but is not complete.

Photoreduction can be minimized by a number of different methods. Most BioXAS experiments keep samples at cryogenic temperatures, which lowers the photoreduction. In order to measure a well defined metal centre, other techniques are under development.

For example, electrochemical cells can be used for *in situ* XAS experiments. These cells are equipped with three electrodes allowing stabilization of the solution potential at an appropriate value or to vary it by a constant rate in order to perform cyclic voltammetry experiments. The metal oxidation state of reactive redox proteins will be either stabilized during the irradiation or will change progressively depending on the potential (Dewald *et al.*, 1986; Ascone *et al.*, 1999; Cognigni *et al.*, 2001).

Stopped/continuous flow devices can provide fresh protein solution at the beam spot.

In some beamlines a shutter has been coupled to the data collection system to prevent sample irradiation when no data are measured. This limits sample degradation under the beam.

All these approaches have to be carefully considered in order to choose the most appropriate method to ensure the stability of sample. When appropriate, the measurement of protein activity before and after the sample irradiation is also recommended.

For metalloproteins that are electron paramagnetic resonance (EPR) active or that show a Mössbauer signal it is feasible to prepare XAS samples in a combined sample holder and monitor any changes in the EPR/Mössbauer signal before and after the BioXAS measurement without defrosting the sample (Hwang *et al.*, 2000).

6.5. Low-energy measurements

Measurements at energies lower than 5 keV imply some additional experimental difficulties. At these energies, the absorption of the incident X-ray beam by atmospheric gases is not negligible and the experiments are performed in a vacuum or in an atmosphere of He gas for energies higher than 1300 eV. A vacuum is a serious constraint for biological samples, which are often in an aqueous solution. The absorption of the sample-holder windows attenuates the intensity of the signal. In some cases integration of the cryostat and detector is a means of eliminating the window between the sample and the fluorescence detector. Frozen solutions can be prepared in windowless sample holders. It should be kept in mind that such a preparation results in lyophilization of the protein, which can alter the metal coordination.

6.6. Sample preparation

As stated in §2, samples can be measured in whatever physical state is available and appropriate. In many low-temperature experiments, 10–30% glycerol is routinely added to the buffer systems as a cryoprotectant. Glycerol is not always appropriate as it can interact with some buffer systems and perturb the pH.

For investigations that do not require kinetic studies in solution, the protein can be embedded in a saccharose solid matrix (Ascone, Sabatucci *et al.*, 2000), protecting the system from X-ray damage and from cryodenaturation.

Mylar or Kapton film is frequently used as a window material for sample cells (as well as cryostats). For ultra-dilute systems the trace amount of metals in the window material (or even the cell or glue used) may be significant (see Ranieri-Raggi *et al.*, 2003), thus

Figure 3
Room-temperature spectra of oxidized (dotted line) and reduced (continuous line) Cu, Zn SOD recorded at DCI-D21 (LURE, Orsay) compared with oxidized Cu, Zn SOD (dashed line) recorded on beamline ID26 at ESRF.

Table 2
The main BioXAS user facilities available at present or in project (check synchrotron web pages for updates).

BM: bending magnet; D: 100% of beam time dedicated to BioXAS applications; P: beamline partially dedicated to BioXAS experiments; MP: multi-purpose set-up.

Country	Synchrotron	Beamline	Energy (keV)	BioXAS activity
BioXAS beamlines				
France	DCI	BM–D21	2.5–30	P
Germany/Europe	DORIS III	BM EMBL	6–30	D
UK	Daresbury	Wiggler-16.5 (sagittal)	9–40	MP
UK	Daresbury	BM-7.1 (sagittal)	4–11	P
USA	SSRL	BL9-3 wiggler	4.6–40	D
USA	SSRL	BL7-3 wiggler	2.4–35	D
USA	SSRL	BL6-2 wiggler	2–32	P†
High-flux beamlines for ultra-diluted samples				
France/Europe	ESRF	ID26	3.2–30	MP
Japan	SPring-8	BL10XU undulator	6–35	MP
USA	APS	18-ID undulator	4–40	MP
Projects of BioXAS beamline				
USA	ALS‡	9.3.1	2–4	P
UK	Diamond	BL C (BM)	2–35	MP
France	Soleil	BM	4–40	P
Italy	DAΦNE-Light§	DXR1 wiggler	1–7	P

† 67%.   ‡ *ALS News* (1999), Vol. 127.   § http://www.lnf.infn.it/esperimenti/sr_dafne_light/.

requiring careful control measurements (even for more concentrated samples running a control sample with buffer is recommended).

Some biological research projects attempt to investigate the structure of pathogenic proteins. At present, to the authors' knowledge, only one example of BioXAS has been performed on samples with a significant biohazard: truncated recombinant prion protein (Hasnain *et al.*, 2001). In this case the samples were brought to the beamline in sealed double-windowed cells and during data collection a strict safety protocol was observed. Experiments on highly pathogenic proteins need P2 or P3 standards. Specific sample holders have to be developed for these systems.

7. Present and future BioXAS centres

As already pointed out in the previous paragraphs, biological XAS requires specific equipment. To further develop the technique as a tool for biologists, user-friendly beamlines with a high level of automation should be developed, allowing users to concentrate on biological issues. The list and description of beamlines, fully or partially dedicated to BioXAS measurements, is summarized in Table 2. We have indicated only existing XAS beamlines used for BioXAS experiments for more than about 10% of the available beam time, high-flux beamlines specific for ultra-dilute samples and projects of beamlines for which BioXAS applications were explicitly mentioned by the project leader.

At present, in a number of national synchrotron radiation sources, it is planned to perform BioXAS experiments on partially dedicated beamlines. A coordination among the different BioXAS national projects could specialize the various beamlines for specific project categories.

8. Conclusion

Metalloprotein studies require optimized beamlines having intense synchrotron photon flux, stable optics, sensitive fluorescence detectors, linearity of I_0 and I_f signals and varied sample environments. All of the technical improvements have increased the quality of measurements. Information obtained is now more detailed as the

k-range of the EXAFS signal is extended. BioXAS for many research areas will be relatively straightforward to perform and will provide key insight into the structure of metalloproteins. New methods are being developed to control and monitor the samples during data collection.

References

Ascone, I., Castagner, R., Tarricone, C., Bolognesi, M., Stroppolo, M. E. & Desideri, A. (1997). *Biochem. Biophys. Res. Commun.* **241**, 119–121.
Ascone, I., Cognigni, A., Giorgetti, M., Berrettoni, M., Zamponi, S. & Marassi, R. (1999). *J. Synchrotron Rad.* **6**, 384–386.
Ascone, I., Cognigni, A., Le Godec, J. P. & Itié, J. P. (2000). *High Press. Res.* **19**, 277–283.
Ascone, I., Sabatucci, A., Bubacco, L., Di Muro, P. & Salvato, B. (2000). *Eur. Biophys. J.* **29**, 391–397.
Banly, C., Masson, P. & Heremans, K. (2002). *Biochim. Biophys. Acta*, **1595**, 3–10.
Bartlet, D. H. (2002). *Biochim. Biophys. Acta*, **1595**, 367–381.
Bianconi, A., Congiu-Castellano, A., Durham, P. J., Hasnain, S. S. & Phillips, S. (1985). *Nature (London)*, **318**, 685–687.
Chen, J., Christiansen, J., Campobasso, N., Bolin, J. T., Tittsworth, B. C., Hales, B. J., Rehr, J. J. & Cramer, S. P. (1993). *Angew. Chem. Int. Ed. Engl.* **32**, 1592–1594.
Cheng, M.-C., Rich, A. M., Armstrong, R. S., Ellis, P. J. & Lay, P. A. (1999). *Inorg. Chem.* **38**, 5703–5708.
Cognigni, A., Ascone, I., Zamponi, S. & Marassi, R. (2001). *J. Synchrotron Rad.* **8**, 987–989.
Cramer, S. P. (1988). *X-ray Absorption. Principles, Application, Techniques of EXAFS, SEXAFS and XANES*, edited by D. C Konsberger & R. Prins, pp. 257–320. New York: John Wiley and Sons.
Cramer, S. P., Dawson, J. H., Hodgson, K. O. & Hager, L. P. (1978). *J. Am. Chem. Soc.* **23**, 7282–7290.
Cramer, S. P., Tench, O., Yocum M. & George, G. N. (1988). *Nucl. Instrum. Methods*, A**266**, 586–591.
Derbyshire, G. E., Cheung, K. C., Sangsingkeow, P. & Hasnain, S. S. (1999). *J. Synchrotron Rad.* **6**, 62–63.
Dewald, H. D., Watkins, J. W. II, Elder, R. C. & Heineman, W. R. (1986). *Anal. Chem.* **58**, 2968–2975.

Ferraroni, M., Rypniewski, W., Wilson, K. S., Viezzoli, M. S., Banci, L., Bertini, I. & Mangani, S. (1999). *J. Mol. Biol.* **288**, 413–426.

Fiamingo, F. G. & Alben, J. O. (1985). *Biochemistry*, **24**, 7964–7970.

Flank, A. M., Weininger, M., Mortenson, L. E. & Cramer, S. P. (1986). *J. Am. Chem. Soc.* **108**, 1049–1055.

Fourme, R., Ascone, I., Kahn, R., Mezouar, M., Bouvier, P., Girard, E., Lin, T. & Johnson, J. E. (2002). *Structure*, **10**, 1409–1414.

Fourme, R., Kahn, R., Mezouar, M., Girard, E., Hörentrup, C., Prangé, T. & Ascone, I. (2001). *J. Synchrotron Rad.* **8**, 1149–1156.

Garner, C. D. & Charnock, J. M. (1993). *Biomolecular Spectroscopy*, Part B, edited by R. J. H. Clark & R. E. Hester, pp. 317–337. New York: John Wiley and Sons.

Gauthier, C., Goulon, J., Moguiline, E., Rogalev, A., Lechner, P., Strüder L., Fiorini, C., Longoni, A., Sampietro, M., Besch, H., Pfitzner, R., Schenk, H., Tafelmeier, U., Walenta, A., Misiakos, K., Kavadias, S. & Loukas, D. (1996). *Nucl. Instrum. Methods*, A**382**, 524–532.

Gauthier, C., Solé, V. A., Signorato, R., Goulon, J. & Moguiline, E. (1999). *J. Synchrotron Rad.* **6**, 164–166.

George, G. N. (1993). *Curr. Opin. Struct. Biol.* **3**, 780–784.

George, S. J., Lowery, M. D., Solomon, E. I. & Cramer, S. P. (1993). *J. Am. Chem. Soc.* **115**, 2968–2969.

Hasnain, S. S. & Hodgson, K. O. (1999). *J. Synchrotron Rad.* **6**, 852–864.

Hasnain, S. S., Murphy, L. M., Strange, R. W., Grossmann, J. G., Clarke, A. R., Jackson, G. S. & Collinge, J. (2001). *J. Mol. Biol.* **311**, 467–473.

Haumann, M., Pospíšil, P., Grabolle, M., Müller, C., Liebisch, P., Solé, V. A., Neisius, T., Dittmer, J., Iuzzolino, L. & Dau, H. (2002). *J. Synchrotron Rad.* **9**, 304–308.

Holm, R. H., Kennepohl, P. & Solomon, E. I. (1996). *Chem. Rev.* **96**, 2239–2314.

Hwang, J., Krebs, C., Huynh, B. H., Edmondson, D. E., Theil, E. C. & Penner-Hahn, J. E. (2000). *Science*, **287**, 122–125.

Jaklevic, J., Kirby, J. A., Klein, M. P. & Roberstson, A. S. (1977). *Solid State Commun.* **23**, 679–682.

Kappen, P., Troger, L., Materlik, G., Reckleben, C., Hansen, K., Grunwaldt, J.-D. & Clausen, B. S. (2002). *J. Synchrotron Rad.* **9**, 246–253.

Kau, L. S., Spira-Solomon, D. J., Penner-Hahn, J. E., Hodgson, K. O. & Solomon, E. I. (1987). *J. Am. Chem. Soc.* **109**, 6433–6442.

Kramer, U., Cotter-Howells, J. D., Charnock, J. M., Baker, A. J. M. & Smith, J. A. C. (1986). *Nature (London)*, **379**, 635–638.

Lagarde, P. & Flank, A. M. (2002). *Chemical Applications of Synchrotron Radiation*, Vol. 12B, *Advanced Series in Physical Chemistry*, edited by T.-K. Sham, pp. 629–663. Singapore: World Scientific.

Lytle, F. W., Greegor, R. B., Sandstrom, D. R., Marques, E. C., Wong, J., Spiro, C. L., Huffman, G. P. & Huggins, F. E. (1984). *Nucl. Instrum. Methods Phys. Res. A*, **226**, 5542–548.

Madigan, M. T. & Oren, A. (1999). *Curr. Opin. Microbiol.* **2**, 265–269.

Pettifer, R. F. & Hermes, C. (1985). *J. Appl. Cryst.* **18**, 404–412.

Pickering, I. J., Prince, R. C., Divers, T. & George, G. N. (1998). *FEBS Lett.* **441**, 11–14.

Powers, L., Chance, B., Ching, Y. & Angiolillo, P. (1981). *Biophys. J.* **34**, 465–498.

Ranieri-Raggi, M., Raggi, A., Martini, D., Benvenuti, M. & Mangani, S. (2003). *J. Synchrotron Rad.* **10**, 69–70.

Retournard, A., Loss, M., Ascone, I., Goulon, J., Lemonnier, M. & Cortés, R. (1986). *J. Phys. C*, **8**(47), 143–147.

Richwin, M., Zaeper, R., Lützenkirchen-Hecht, D. & Frahm, R. (2001). *J. Synchrotron Rad.* **8**, 354–356.

Rowen, M., Rek, Z., Wong, J., Tanaka, T., George, G. N., Pickering, I. J. & Via, G. H. V. (1993). *Synchrotron Rad. News*, **6**, 25–26.

Scott, R. A., Hahn, J., Doniach, S., Freeman, H. C. & Hodgson, K. O. (1982). *J. Am. Chem. Soc.* **104**, 5364–5369.

Shadle, S. E., Penner-Hahn, J. E., Schugar, H. J., Hedman, B., Hodgson, K. O. & Solomon, E. I. (1993). *J. Am. Chem. Soc.* **115**, 767–776.

Shu, L., Nesheim, J. C., Kauffmann, K., Münck, E., Lipscomb, J. D. & Que, L. Jr (1997). *Science*, **275**, 515–518.

Solé, V. A., Gauthier, C., Goulon, J. & Natali, F. (1999). *J. Synchrotron Rad.* **6**, 174–175.

Tanida, H. & Ishii, M. (2001). *Nucl. Instrum. Methods*, A**467**/**468**, 1564–1567.

Wang, H. X., Patil, D. S., Gu, W. W., Jacquamet, L., Friedrich, S., Funk, T. & Cramer, S. P. (2001). *J. Electron Spectrosc.* **114**, 855–863.

Yu, E. Y., Pickering, I. J., George, G. N. & Prince, R. C. (2001). *Biochim. Biophys. Acta*, **1527**, 156–160.

Zhang, K., Rosenbaum, G. & Bunker, G. (1998). *J. Synchrotron Rad.* **5**, 1227–1234.